On Mass Distribution in ESPResSo Simulations of Elastic Objects*

Iveta Jančigová
Cell-in-fluid Research Group, http://cell-in-fluid.fri.uniza.sk
Faculty of Management Science and Informatics, University of Žilina
Univerzitná 8215/1, 010 26 Žilina, Slovakia
Email: iveta.jancigova@fri.uniza.sk

***Abstract*—Modeling fluid flow with immersed elastic objects gives important insights into various biological phenomena. The recently developed object-in-fluid module of open-source simulation package ESPResSo is very well suited for simulations of such objects. In this article, we outline a procedure, how to properly account for the mass of elastic objects in the simulations where the objects are modeled using surface meshes.**

***Keywords*—elastic object, ESPResSo, mass distribution, object-in-fluid, red blood cell**

I. Introduction

Models of flow with immersed cells are used in simulations that have various biomedical applications, e.g. in simulations of microfluidic devices meant to capture circulating tumor cells from blood [1] or in simulations of devices meant to separate individual cells for subsequent proteomics [2], etc. What these have in common, is that they rely on a model of fluid flow with immersed elastic objects. Our research group has developed a module [3] as part of an open-source simulation package ESPResSo [4] that can be used for simulations of such flow. However, this module cannot be used as a black box, the user has to have an understanding of the underlying models.

The elastic objects are modeled using a surface mesh of points that interact with the fluid. These points have their own mass. In simulations, one often uses different triangulations of the same object, e.g. to increase precision by having larger number of nodes or to reduce the computational cost by having fewer nodes. In these cases, the total mass of the object varies, depending on how many surface points were used.

Intuitively, one could say that this effect is negligible, since most of the mass of the object comes from the inner fluid and the surface membrane in biological cells or surface triangulation in the simulated cells give only a small contribution. In order to illustrate that this is indeed an issue, we present the graph in Fig. 1, which shows velocity profiles of an object coming from the same simulation (described in more detail in the following sections) performed using different triangulations and keeping the mass of individual boundary points constant.

*This work was supported by the Slovak Research and Development Agency under the contract No. APVV-0441-11.

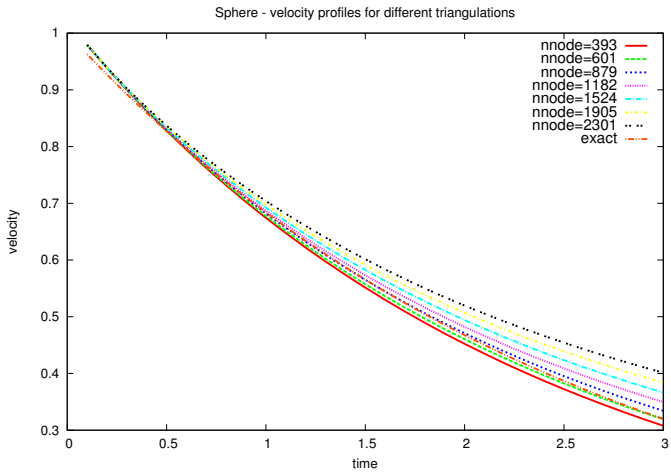

Fig. 1. Not adjusting the mass of immersed boundary points results in different velocity profiles for simulations that differ only by the number of triangulation nodes.

In this article, we investigate how to distribute the mass properly in ESPResSo simulations to avoid this effect.

II. Model

Our model comes from [5]. It comprises two main parts - the fluid and the elastic object. For the fluid, e.g. blood plasma, we use the lattice-Boltzmann method (LBM [6]) briefly described in the next section, because it allows convenient implementation without the necessity to solve partial differential equations (e.g. Navier-Stokes equations). For elastic objects, e.g. the red blood cells, we use a spring network model, in which the spring network forms a surface triangulation of the object. These two models are connected using the immersed boundary method.

A. Lattice-Boltzmann method for the fluid

The LBM uses a fixed regular 3-dimensional grid and represents the fluid domain by a set of lattice nodes. The fluid itself is modeled as a group of fictitious fluid particles that are only allowed to either stay where they are or move to the

neighboring nodes. The state of the fluid at a given node $\mathbf{x}$ at time t is described by distribution functions $f_a(\mathbf{x}, t)$, where a represents the directions to 18(+1) neighboring nodes. The governing equations are

$$\underbrace{f_a(\mathbf{x} + \mathbf{e}_a\delta_t, t + \delta_t) = f_a(\mathbf{x}, t)}_{propagation} - \underbrace{\Delta_a(\mathbf{f}(\mathbf{x}, t))}_{collision} \quad (1)$$

where $\mathbf{e}_a$ are the velocity vectors pointing to the adjacent nodes, δ_t is the time step and Δ_a denotes the collision operator that accounts for the difference between pre- and post-collision states and satisfies the constraints of mass and momentum conservation.

The macroscopic quantities, velocity $\mathbf{u}$ and density ρ, are evaluated from

$$\rho(\mathbf{x}, t) = \sum_a f_a(\mathbf{x}, t) \qquad \text{and} \qquad \rho(\mathbf{x}, t)\mathbf{u} = \sum_a f_a(\mathbf{x}, t)\mathbf{e}_a.$$

B. Elastic model of the object

Our primary objects of interest are red blood cells and therefore the elastic properties that we need captured in the model are resistance of the membrane to surface dilation, viscoelastic resistance to bending and stretching of the membrane and total volume conservation. Details of this model can be found in [7].

For simplicity and clarity, we also perform analysis and simulations using spheres that have the same characteristics. The stretching elasticity of such sphere has already been analyzed to some extent in [8], discussion of scalability of forces can be found in [9] and an alternative approach considering energies corresponding to the elastic forces is in [10].

C. Coupling fluid and objects - Immersed boundary method

For the motion of the spring network nodes (immersed boundary points - IBP) we use the Newton equation

$$m_{IBP}\mathbf{x}_j'' = \mathbf{F}_j, \quad (2)$$

where $\mathbf{x}_j$ is the position of the given node. The nodes and the fluid influence each other, so in order to couple the two equations of motion, we assume the force exerted by the fluid on one IBP to be proportional to the difference of the velocity $\mathbf{v}$ of the IBP and the fluid velocity $\mathbf{u}$ at the same position:

$$\mathbf{F}_{jf} = \xi(\mathbf{v} - \mathbf{u}). \quad (3)$$

Since the grid points and immersed boundary points do not coincide, we use interpolation to obtain the needed values. Note that $\mathbf{F}_j = \mathbf{F}_{jf} + \mathbf{F}_{je}$, where $\mathbf{F}_{je}$ is the composition of all elastic forces acting on node j.

III. Theoretical analysis

A. Biological values

A typical healthy red blood cell has the density $\rho_{RBC} \approx 1.11\frac{g}{mL}$ and mass $m_{RBC} \approx 110pg$ [11], The resulting volume is thus $V_{RBC} \approx 99\mu m^3$. The authors in [11] observe that the intrinsic cell-to-cell variation in density is nearly 100-fold smaller than the mass or volume variation.

Thickness of the red blood cell membrane is $h_{RBC} \approx 40nm$ [12] and the density of blood plasma $\rho_{plasma} = 1.025\frac{g}{mL}$ [13].

B. Sphere

In this analysis, we first consider a sphere with density $\rho = \rho_{RBC} = 1.11\frac{g}{mL}$, diameter $r = 4\mu m$ and membrane thickness $h = 40nm$. Thus, the mass of this object is

$$m = \rho V = \rho\frac{4}{3}\pi r^3 = 1.11\frac{g}{mL}\frac{4}{3}\pi(4\mu m)^3 \approx 297.6pg \quad (4)$$

In our model, this mass consists of two parts. One is the mass of inner cytoplasm, which is modeled using the same fluid as the blood plasma in which the cell is moving, and the mass of the "membrane", which consists of the immersed boundary points. More specifically:

$$m = m_{inside} + m_{membrane} = \rho_{plasma}\frac{4}{3}\pi(r - h)^3 + Nm_{IBP} \quad (5)$$

where N is the number of IBPs (number of triangulation nodes) and m_{IBP} is the mass of each IBP. Both of these quantities are set for each simulation.

Combining equations (4) and (5), we get

$$m_{membrane} = Nm_{IBP} \approx 31pg \quad (6)$$

In our model, this is the mass of object's membrane and should be equally distributed among the N triangulation nodes, e.g. for a triangulation with 500 surface nodes, the mass of each node is

$$m_{500} = \frac{m_{membrane}}{500} \approx 0.062pg.$$

C. Red blood cell

The calculation is more difficult for the red blood cell because we do not have a simple formula for its volume. Therefore, we make a simplifying assumption that the membrane has zero thickness. This simplification is quite reasonable for our model, because we do not specifically model the membrane and so the inner fluid "fills the whole object". Thus, we have

$$m_{RBC} = m_{inside} + m_{membrane}$$

and we compute m_{inside} as

$$m_{inside} = \rho_{plasma}V_{RBC}$$

We then get $m_{membrane} = 110pg - 1.025\frac{g}{mL}99\mu m^3 = 8.4pg$. This is an approximation of the mass that should be equally distributed among the N triangulation nodes.

IV. Simulation results

In this section, we present the results of two kinds of simulations that correspond to the analysis in previous section. One set concerns spheres and the other red blood cells.

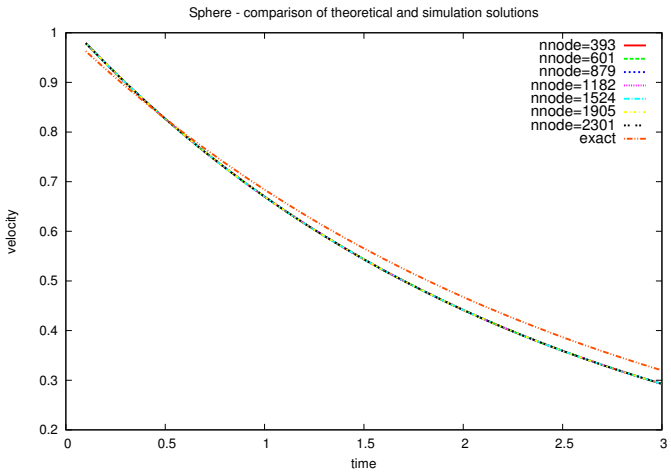

Fig. 2. Velocity profiles for different sphere triangulations are nearly identical and correspond well to the analytical solution, when the mass of IBPs is adjusted.

A. Sphere

The main reason to include simulations with spheres is that there are known theoretical results for spheres in flow that we can compare to. The sphere is immersed in a stationary fluid and given an initial velocity (in the x-direction) $v_0 = 1\frac{Lm}{Ls} = \frac{m}{s}$. The fluid slows it down until it stops.

The theoretical solution to this problem can be computed as follows. Stokes drag force exerted on a sphere is $F_d = -6\pi\nu r v K$. For sphere, the shape factor $K = 1$, r is the radius. ν is the dynamic viscosity of the fluid and v is the velocity of the sphere. The equation of motion for the sphere is

$$mx'' = F$$

so by setting $F = F_d$ we get

$$mv' + 6\pi\nu r v = 0$$

This is a first order ordinary differential equation. With initial condition $v(0) = v_0$, we get an analytical solution for the velocity $v_{ex}(t) = v_0 e^{-\frac{6\pi\nu r K}{m}t}$.

In simulations, we took a sphere with diameter 4μm. The mass of the sphere was set to $297.6pg = 297.6Lkg = 297.6 \times 10^{-15}kg$ (as computed in section III-B). The membrane portion of the mass was then equally divided among the nodes of surface triangulation. The triangulations that were used had 393, 601, 879, 1182, 1524, 1905 and 2301 nodes. So, in the 393 triangulation, each particle had the mass $m_{IBP} = \frac{31}{393} \approx 0.079pg$ and in the 2301 triangulation, each particle had the mass $m_{IBP} = \frac{31}{2301} \approx 0.013pg$. Viscosity was $\nu = 0.0015\frac{kg}{ms}$.

It needs to be pointed out, that there is another simulation parameter - friction coefficient ξ - that is linked to the m_{IBP} by equations (2) and (3). When the m_{IBP} is doubled, also ξ needs to be doubled in order to achieve the same dynamics. In our simulations, we have adjusted ξ according to varying m_{IBP}.

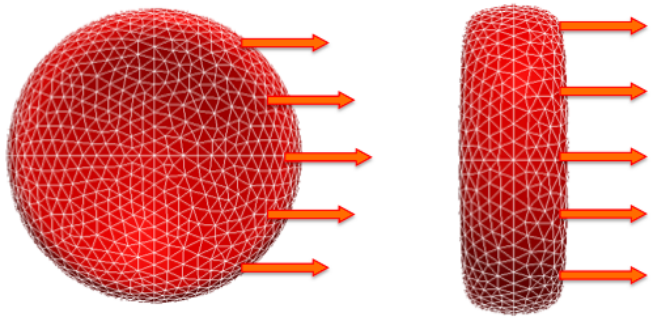

Fig. 3. In one set of simulations, the cell's smallest profile was in the direction of applied velocity (on the left) and in the other set of simulations, the cell was facing the direction of applied velocity (on the right). This visualization was created using open source analysis and visualization application ParaView [14].

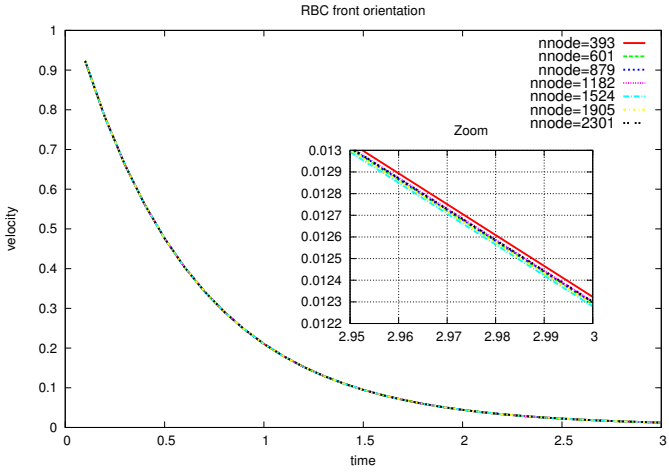

Fig. 4. Red blood cell with various surface triangulations was immersed in a stationary fluid "facing" the direction of its initial velocity. Mass of IBPs was properly adjusted. The velocity profiles are nearly identical. The relative error $\frac{v_{393}-v_{2300}}{v_{2300}} = 0.19\%$ at the time $t = 3$.

In Fig. 2, the theoretical velocity profile is compared to velocities obtained in simulations. We see that these profiles obtained using properly adjusted m_{IBP} correspond well to the theoretical result and, unlike in Fig. 1, are nearly identical. The small deviation from analytical solution might be due to the fact, that we simulate an elastic object and not a rigid sphere and perhaps a not optimal selection of baseline ξ.

B. Red blood cell

For red blood cells, we do not have a theoretical solution to compare to, but we can compare the different triangulations to each other. We have performed two sets of simulations. In both, an RBC is immersed in a stationary fluid and given an initial velocity in the x-direction $v_0 = 1\frac{Lm}{Ls} = \frac{m}{s}$. The fluid slows it down until it stops. The difference between the two sets of simulations is in the spatial orientation of the cell - see Fig. 3. In one case the cell was "facing" the

direction of initial velocity, in the other it was rotated so that its smallest profile presented in the direction of initial velocity.

We again used different triangulations and results for one set of the simulations are displayed in Fig. 4. We see that the change of triangulation has a minimal effect on the velocity profile. We are not showing the other set of results because level of achieved correspondence among triangulations is very similar.

V. Conclusion

As demonstrated by the theoretical check and simulations, the proper procedure to account for the mass of immersed boundary points in ESPResSo simulations of elastic objects is to check the mass of the inner fluid, then determine the mass of the membrane and finally distribute this mass into the Immersed boundary points. In the simulations, the friction coefficient ξ needs to be adjusted accordingly.

Acknowledgement

The author would like to thank Ivan Cimrák, Hynek Bachratý and Katarína Bachratá for their insightful comments.

References

[1] S. Nagrath, L. V. Sequist, S. Maheswaran, D. W. Bell, D. Irimia, L. Ulkus, M. R. Smith, E. L. Kwak, S. Digumarthy, A. Muzikansky, P. Ryan, U. J. Balis, R. G. Tompkins, D. A. Haber, and M. Toner, "Isolation of rare circulating tumour cells in cancer patients by microchip technology," *Nature*, vol. 450, pp. 1235–1239, 2007.

[2] A. Salehi-Reyhani, J. Kaplinsky, E. Burgin, M. Novakova, A. J. deMello, R. H. Templer, P. Parker, M. A. A. Neil, O. Ces, P. French, K. R. Willison, and D. Klug, "A first step towards practical single cell proteomics: a microfluidic antibody capture chip with TIRF detection," *Lab Chip*, vol. 11, pp. 1256–1261, 2011. [Online]. Available: http://dx.doi.org/10.1039/C0LC00613K

[3] I. Cimrák, M. Gusenbauer, and I. Jančigová, "An ESPResSo implementation of elastic objects immersed in a fluid," *Computer Physics Communications*, vol. 185, no. 3, pp. 900 – 907, 2014.

[4] A. Arnold, O. Lenz, S. Kesselheim, R. Weeber, F. Fahrenberger, D. Roehm, P. Košovan, and C. Holm, "ESPResSo 3.1 - molecular dynamics software for coarse–grained models," in *Meshfree Methods for Partial Differential Equations VI, Lecture Notes in Computational Science and Engineering*, M. Griebel and M. Schweitzer, Eds., vol. 89, 2013, pp. 1–23.

[5] M. Dupin, I. Halliday, C. Care, and L. Alboul, "Modeling the flow of dense suspensions of deformable particles in three dimensions," *Phys Rev E Stat Nonlin Soft Matter Phys.*, vol. 75, p. 066707, 2007.

[6] B. Dunweg and A. J. C. Ladd, "Lattice Boltzmann simulations of soft matter systems," *Advances in Polymer Science*, vol. 221, pp. 89–166, 2009.

[7] I. Cimrák, M. Gusenbauer, and T. Schrefl, "Modelling and simulation of processes in microfluidic devices for biomedical applications," *Computers and Mathematics with Applications*, vol. 64, no. 3, pp. 278 – 288, 2012.

[8] I. Cimrák, I. Jančigová, K. Bachratá, and H. Bachratý, "On elasticity of spring network models used in blood flow simulations in ESPResSo," in *III International Conference on Particle-based Methods – Fundamentals and Applications PARTICLES 2013*, M. Bisschoff, E. Oñate, D. Owen, E. Ramm, and P. Wriggers, Eds., 2013, pp. 133–144.

[9] I. Jančigová and R. Tóthová, "Scalability of forces in mesh-based models of elastic objects," 2014, preprint, accepted for publication at 10th International Conference ELEKTRO 2014.

[10] R. Tóthová, I. Jančigová, and I. Cimrák, "Energy contributions of different elastic moduli in mesh-based modeling of deformable object," 2014, preprint, accepted for publication at 10th International Conference ELEKTRO 2014.

[11] W. H. Grover, A. K. Bryan, M. Diez-Silva, S. Suresh, J. M. Higgins, and S. R. Manalis, "Measuring single-cell density," *Proceedings of the National Academy of Sciences*, 2011. [Online]. Available: http://www.pnas.org/content/early/2011/06/15/1104651108.abstract

[12] V. Heinrich, K. Ritchie, N. Mohandas, and E. Evans, "Elastic thickness compressibility of the red cell membrane," *Biophys J.*, vol. 81, no. 3, p. 14521463, Sep 2001, PMCID: PMC1301624.

[13] R. J. Trudnowski and R. R. C., "Specific gravity of blood and plasma at 4 and 37 degrees C," *Clin Chem.*, vol. 20, no. 5, pp. 615–6, May 1974.

[14] A. Henderson, "ParaView guide, A Parallel Visualization Application," Kitware Inc., Tech. Rep., 2007.